ISSN 1063-7834, Physics of the Solid State, 2017, Vol. 59, No. 9, pp. 1852–1866. © Pleiades Publishing, Ltd., 2017.
Original Russian Text © A.M. Latyshev, A.V. Bakulin, S.E. Kulkova, 2017, published in Fizika Tverdogo Tela, 2017, Vol. 59, No. 9, pp. 1828–1842.

SURFACE PHYSICS, THIN FILMS

Adsorption of Oxygen on Low-Index Surfaces of Ti_3Al Alloy

A. M. Latyshev[a, b], A. V. Bakulin[a, b, *], and S. E. Kulkova[a, b]

[a] *Institute of Strength Physics and Materials Science, Siberian Branch, Russian Academy of Sciences, Tomsk, 634055 Russia*

[b] *Tomsk National Research State University, Tomsk, 634050 Russia*

**e-mail: bakulin@ispms.tsc.ru*

Received February 14, 2017

Abstract—The atomic and electronic structure of the three surfaces of Ti_3Al alloy—(0001), $(1\bar{1}00)$, and $(11\bar{2}0)$—is calculated by the projector augmented-wave method in the framework of the electron density functional theory. The surface energies are estimated as a function of the chemical potential of aluminum, which made it possible to construct a stability diagram for the surfaces under study. Adsorption of oxygen on differently oriented surfaces of the alloy is studied. It is found that the most preferred positions for oxygen adsorption are hollow positions on the (0001) and $(11\bar{2}0)_{Ti-Al}$ surfaces and bridge positions on the $(1\bar{1}00)_{Ti-Al\text{-}1}$ surface. Structural and electronic factors that determine these energy preferences are discussed. It is shown that regardless of the orientation of the surface, oxygen "prefers" titanium-enriched positions. The effect of oxygen on the atomic and electronic structure of low-index surfaces is discussed. It is found that at low concentrations of oxygen, the formation of its chemical bond with titanium and/or aluminum atoms in the surface and subsurface layers leads to the appearance of low-lying states split off from the bottom of the valence bands of metals, which is accompanied by the formation of a pseudogap and the weakening of Ti–Al metal bonds in the surface layers.

DOI: 10.1134/S1063783417090165

1. INTRODUCTION

Titanium aluminides are widely used in the aerospace, aviation, and automotive industries due to their good mechanical properties, in particular, high specific strength and melting point, high elastic modulus, elasticity, and heat resistance [1–3]. Despite intensive experimental and theoretical study over the past decades, these intermetallic alloys still attract the attention of researchers from both a technological and a fundamental point of view. At the same time, the insufficient corrosion resistance of Ti_3Al and TiAl alloys limits their use at high temperatures, and $TiAl_3$, which shows maximum resistance to oxidation, is rather brittle. The development of new high-temperature structural materials based on Ti–Al alloys is an important task of modern materials science. Experimental studies [4–7] have shown that low corrosion resistance of alloys with a lower aluminum concentration is associated with the growth of mixed oxide layers containing titanium and aluminum oxides. It is known that continuous oxide layers formed on the surface are effective barriers for the diffusion of oxygen, which limits the growth rate of oxide films even at high temperatures [4–7]. In this regard, it is necessary to understand the microscopic mechanisms of oxidation of Ti–Al alloys depending on their composition and the features of the interaction of oxygen with atoms in surface layers, which will allow to establish the main factors affecting the growth kinetics of oxide layers and their properties. It is known that the formation energies of TiO_2 and Al_2O_3 are –9.78 and –11.58 eV, respectively [8]. It is believed that a metal that has a higher energy of oxide formation in modulus is oxidized first and segregates to the surface even at low temperatures and low oxygen concentrations. In addition, titanium can be oxidized to form a series of oxides (Ti_2O, TiO, Ti_2O_3, Ti_3O_5, or TiO_2), while aluminum does not form intermediate oxide phases, and Al_2O_3 is found on the surface of Ti–Al alloys even at low temperatures. Therefore, titanium can play an important role in the formation of oxide films on the surface of alloys, depending on its concentration. It is rather difficult to obtain experimentally information at a microscopic level about the initial stage of oxidation of the alloy surface due to the effect of various factors on this process, such as the presence of impurities, the surface structure, the capabilities of experimental methods, and their conditions. Therefore, the importance of theoretical approaches increases, for example, the methods within the electron density functional theory (DFT), which enables one to obtain the values of the oxygen binding energies for different

positions on the alloy surface, depending on its orientation.

Compared to the metal surfaces for those the oxidation mechanisms were intensively studied by theoretical methods, intermetallic alloys gained less attention. One of the first theoretical papers devoted to the study of the processes of oxidation of the surface of alloys is the publication of Lozovoi et al. [9], in which the adsorption of oxygen on the NiAl(110) surface is studied. At present, several papers [10–20] are known in that low-index Ti–Al surfaces alloys and their interaction with oxygen are considered, with γ-TiAl alloy to be the studied. In [10, 11], adsorption of oxygen on the γ-TiAl(111) surface was investigated. It was demonstrated that the positions most enriched with titanium were the most preferable for oxygen adsorption, and the formation of metal–oxygen bonds led to a weakening of the metal bond in the alloy. We note that the effect of the oxygen concentration on the atomic structure of the (111) surface was also considered in [10]. In particular, it was found that oxygen, being introduced into the subsurface layer, led to the formation of mixed disordered oxide layers with significant structural distortions. It was noted that annealing could help to stabilize the surface oxide and to improve its ordering. The effect of segregation on the adsorption of oxygen on the γ-TiAl(111) surface was studied in [11]. The authors showed that segregation of aluminum lowered the surface energy, while the adsorption of oxygen on the surface with two antistructural Al defects (Al-antisite) was similar to adsorption on the corresponding surface of pure aluminum, and the binding energy of oxygen with the surface decreased with increasing its concentration. The stability of the low-index surfaces of the γ-TiAl alloy was studied in [12]. In addition, the adsorption of oxygen on other surfaces of the γ-TiAl alloy ((001), (100), and (110)) was studied in [13–16]. For example, it was determined in [13] that the most preferable position for the adsorption of oxygen on the TiAl(001) surface terminated with titanium is a top-position above the titanium atom of the surface layer (T_{Ti}), whereas in [14–16], it was found that the hollow position above the aluminum atom of the subsurface layer (H_{Al}) was preferred. In addition, the diffusion of oxygen both in the bulk of the alloy and from the surface into the bulk of the material was studied in our previous papers [15, 16]. According to our information, there is only one paper [17] in that the adsorption of oxygen on the surface of the $TiAl_3$ alloy was investigated. In this paper, the surface energies of low-index surfaces are calculated in dependence on their termination, and it is demonstrated that the priority of oxidation of aluminum over titanium is observed on aluminum-terminated (001) and (110) surfaces. At the mixed termination of these surfaces, the interaction with aluminum prevails over titanium oxidation only at low oxygen concentrations up to 1.5 monolayers, which is consistent with experiment [1].

There are several papers [18–20], in which microscopic mechanisms of oxidation of the stoichiometric $Ti_3Al(0001)$ surface are studied. In [18], an analysis of the effect of antistructural defects on the energy stability of a given surface was made, including with an increase in the oxygen concentration. It was found that the $Ti_3Al(0001)$-3Al surface with three aluminum defects in the surface layer was the most stable in the limit of high aluminum concentrations. The authors showed that the adsorption of oxygen enhanced the segregation of aluminum to the surface and confirmed the formation of a two-phase oxide system, which agreed with the experiment [21]. Adsorption of molecular oxygen on the stoichiometric $Ti_3Al(0001)$ surface was also studied [19]. It was shown that oxygen molecules mainly dissociated, with oxygen atoms tending to occupy the most energetically preferred hollow positions on the $Ti_3Al(0001)$ surface. In the subsequent work of these authors [20], adsorption of atomic oxygen on the same surface was considered, including with an increase in the coverage degree oxygen to one monolayer. Generally, it is demonstrated in [19, 20] that the highest binding energy of oxygen with the surface corresponds to the positions in that the oxygen adatom forms bonds primarily with titanium atoms. At the same time, the stability of the low-index surfaces of the Ti_3Al alloy was not discussed in the early papers mentioned above, and the adsorption of oxygen on other surfaces was not studied.

Thus, the goal of this work is a comparative study of oxygen binding energy on three low-index surfaces: (0001), $(1\bar{1}00)$, and $(11\bar{2}0)$, which will yield new insights into the mechanisms of oxygen bonding on differently oriented surfaces, depending on the composition of the surface layers and, as a consequence, the initial stage of oxidation of the Ti_3Al alloy surface.

2. METHOD OF CALCULATION

The atomic and electronic structure of the low-index surfaces of the Ti_3Al alloy was calculated by the projector augmented-wave (PAW) method in the plane-wave basis [22, 23], implemented by the VASP code [24–26], with the generalized gradient approximation for the exchange-correlation functional in the form of GGA–PBE [27]. The maximum energy of plane waves from the basic set was 550 eV. When calculating the electronic structure of a bulk alloy, integration over the Brillouin zone was carried out using a Γ-centered grid of $13 \times 13 \times 17$ k-points. Convergence was considered achieved if the difference in total energies for the next two iterations did not exceed 10^{-5} eV.

To calculate the surface energy of the low-index surfaces of the Ti_3Al alloy with different orientations, the approach of multilayer symmetric films separated by a vacuum gap of at least 15 Å was used. For each surface, the optimal number of atomic layers in the film was determined by the test calculations of surface

energy, which showed that an increase in the number of layers in the film above 9, 14, and 16 for surfaces (0001), $(11\bar{2}0)$, and $(1\bar{1}00)$, respectively, did not lead to significant changes in the surface energy, and the accuracy of calculating the surface energy was ~0.005 J/m^2. The relaxation of the atomic positions of the surface layers was carried out using Newton's dynamics until the forces on atoms were less than 0.01 eV/Å. In the case of the (0001) surface, a Γ-centered grid of $7 \times 7 \times 1$ k-points was used, and a grid of $5 \times 7 \times 1$ k-points, generated by the Monkhorst–Pack method [28] was used to calculate surfaces with orientation $(11\bar{2}0)$ and $(1\bar{1}00)$.

Adsorption of oxygen on the low-index surfaces of the Ti_3Al alloy was studied in the model of asymmetric films described in our early paper [16]. Note that oxygen can be adsorbed at various positions on the alloy surface, depending on its orientation. As a rule, we consider high-symmetry positions in voids coordinated by three to four surface atoms (hollow), between two atoms (bridge), and above surface atoms (top). Atoms of the three layers on the underside of the film were fixed in positions corresponding to bulk ones, while the positions of the atoms of the remaining layers were optimized. The adsorption energy of an oxygen atom was calculated by equation

$$E_{ads} = -[E_{O/Ti_3Al} - E_{Ti_3Al} - (1/2)E_{O_2}], \quad (1)$$

where E_{O/Ti_3Al} and E_{Ti_3Al} are the total energy of the surface with oxygen and without it, and E_{O_2} is the total energy of an oxygen molecule, calculated in an empty cell with dimensions $12 \times 12 \times 12$ Å. Factor 1/2 corresponds to the adsorption of oxygen on one surface of the alloy. The binding energy of oxygen on the surface was calculated as

$$E_b = -[E_{O/Ti_3Al} - E_{Ti_3Al} - E_O], \quad (2)$$

where E_O is the total energy of the oxygen atom. It is known that in the spin-polarized calculation, the binding energy in the oxygen molecule is ~1 eV [15, 29] higher than the experimental value (5.12 eV [30]). In order to compensate for the inaccuracy of the calculations, the experimental value of the binding energy is often used in the estimates of the oxygen adsorption energies within the DFT. In this approach, the total energy of the oxygen molecule in our calculation is 8.23 eV. Note that the theoretical value of the energy of an oxygen molecule of 9.86 eV agrees well with the value of 9.80 eV obtained in [11].

3. RESULTS AND DISCUSSION

3.1. Properties of Ti_3Al Bulk Alloy

The Ti_3Al alloy has a hexagonal close-packed structure of the $D0_{19}$ type, shown in Fig. 1, which is characterized by the space group 194. The calculated parameters of the alloy lattice (a and c) for the ground state, the elastic constants C_{ij}, and the bulk modulus B are given in Table 1. Comparison of the theoretical lattice parameters with the available data shows that they differ from the experimental values by less than 0.6%. The elastic constants show a slight deviation from the values obtained in the early calculations [31, 32] using other methods within the DFT and are in good agreement with the experimental data [34], measured at 3.3 K and extrapolated to zero temperature. As shown in [34], the elastic constants change by 1.3–6.2% with an increase in temperature up to 270 K. We note that the theoretical elastic constants of alloys differ from the experiment in the range of 5–12%, and their values depend strongly on the approximation for the exchange-correlation functional and the number of k-points, over which the integration over the Brillouin zone is carried out. It is known that the value of the bulk modulus depends on the method of its calculation. If B is estimated by the Murnaghan equation [35] using total energies calculated as a function of the volume of the alloy, then its value agrees better with the experiment than the estimate for elastic constants. The electron energy spectrum and the densities of the electronic states of the Ti_3Al alloy are similar to those given in the earlier papers [36–38] and therefore are not discussed. Calculations of the structural and electronic properties of the alloy indicate the adequacy of the method and give us a hope that its use for calculations of oxygen adsorption in the bulk of the alloy and on its surfaces yields reliable results.

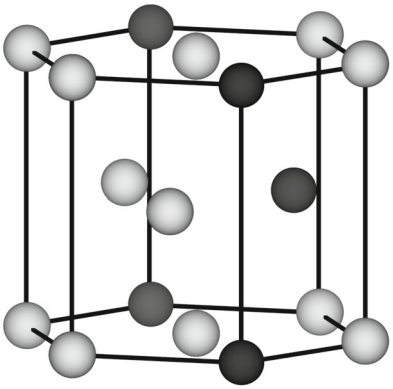

Fig. 1. Atomic structure of α_2-Ti_3Al alloy. Atoms of titanium and aluminum are shown by light and solid balls, respectively.

The oxygen absorption energy calculated by a formula similar to Eq. (1) in the Ti_3Al alloy in octahedral (O) and tetrahedral positions is in good agreement with the results of the theoretical work [39]. The energy of oxygen absorption in the most preferred $O1$-position is 6.22 eV (6.23 eV [39]). This position has only titanium atoms among nearest neighbors, while a smaller value of 1.54 eV was obtained for the $O2$-position, which is located in the octahedron formed by four

Table 1. Lattice parameters and elastic moduli of Ti_3Al alloy in comparison with available experimental and theoretical data

Parameter	Our calculation	Calculation [31]	Calculation [32]	Experiment
a, Å	5.736	5.72	5.64	5.77*
c, Å	4.639	4.63	4.57	4.62*
c/a	0.809	0.81	0.81	0.80*
C_{11}, GPa	193	185	221	183**
C_{12}, GPa	90.7	83	71	89.1**
C_{13}, GPa	66.6	63	85	62.6**
C_{33}, GPa	235.8	231	238	225*
C_{44}, GPa	55.5	57	69	64.1**
C_{66}, GPa	51.1	61	75	47.0**
B, GPa	118.8	–	129	113**

*Data [33].
**Data [34].

titanium atoms and two aluminum atoms. The absorption of oxygen in the tetrahedral position, when the aluminum atom is at its base, leads to its shift to the hexahedral position, in which it is in the basal plane in the triangle formed by two titanium atoms and one aluminum atom, with the absorption energy only 0.10 eV lower than in the *O*2-position. When absorbed in a tetrahedron with aluminum at its vertex, the oxygen atom is not displaced, and its absorption energy is 3.77 eV (3.83 eV [39]). Note that experimental studies using neutron diffraction [40] also indicate that oxygen atoms preferentially occupy octahedral *O*1-positions.

3.2. Energy Stability of Low-Index Ti_3Al Surfaces

Figure 2 demonstrates the atomic structure of the three examined surfaces of the Ti_3Al alloy. The surface (0001) has the stoichiometric composition (Fig. 2a), whereas for the surfaces $(11\bar{2}0)$ and $(1\bar{1}00)$, two and four types of termination are possible, respectively (Figs. 2b and 2c). For example, $Ti_3Al(1\bar{1}00)$ can be terminated with both an atomic layer of titanium and a mixed layer of Ti–Al, and the composition of the subsurface layer can also be different. Therefore, if the surface and subsurface layers are formed by titanium atoms, then such a termination is denoted Ti-2, and in the case of a mixed subsurface layer, this termination of the surface is denoted Ti-1. A similar approach is also used in the case of a mixed surface layer. Thus, the index (Ti or Ti–Al) indicates with what kind of atomic layer the surface is terminated.

Surface energy was calculated using the conventional equation of

$$\sigma = \frac{1}{2S}[E_{tot}^{slab} - N_{Ti}\mu_{Ti_3Al} - \mu_{Al}^{bulk}(3N_{Al} - N_{Ti}) - \Delta\mu_{Al}(3N_{Al} - N_{Ti})], \quad (3)$$

where N_{Ti} and N_{Al} are the number of titanium and aluminum atoms in the alloy film, μ_{Ti_3Al} is the chemical potential of the bulk alloy, and $\Delta\mu_{Al}$ is the deviation of the chemical potential of aluminum on the Ti_3Al surface from its value in bulk aluminum (μ_{Al}^{bulk}), which can vary in the range of $-\Delta H \le \Delta\mu_{Al} \le 0$, where ΔH is the enthalpy of formation of Ti_3Al; $\Delta H = 1.125$ eV. The calculated value of ΔH agrees well with the experimental data (1.00–1.16 eV [41–43]) and theoretical values (1.13 [18] and 1.160 eV [20]). More details of the calculation of surface energy are given in our earlier works [15, 16].

The calculated stability diagram of the low-index surfaces of the Ti_3Al alloy is presented in Fig. 3. It is seen that the $(11\bar{2}0)_{Ti-Al}$ surface with a mixed termination is stable in the Al-enriched region, whereas the $(1\bar{1}00)_{Ti-Al-1}$ surface with a mixed termination is more stable in the Ti-enriched limit. The difference in the surface energies of this structure and the basal stoichiometric surface (0001) is minimal; it is 0.012 J/m^2. The large stability of surfaces, the upper layer of which contains aluminum atoms, is consistent with the previously revealed trends for TiAl and $TiAl_3$ alloys [11, 12, 14–17]. The calculated surface energy of the basal plane (0001) is 1.987 J/m^2, which agrees well with the results of early studies: 1.964 [44] and 2.02 J/m^2 [39]. The energies of other surfaces were not previously calculated.

Table 2 shows the relaxation of the first three interlayer distances and the splitting of the mixed layer nearest to the surface: the first layer in the case of (0001), $(11\bar{2}0)_{Ti-Al}$, $(1\bar{1}00)_{Ti-Al-1}$, and $(1\bar{1}00)_{Ti-Al-2}$; the second layer for $(11\bar{2}0)_{Ti}$ and $(1\bar{1}00)_{Ti-1}$; and the third layer for $(1\bar{1}00)_{Ti-2}$ surface. The relaxation of the interlayer distances is estimated by equation $\Delta d_{ij} = (d_{ij} - d_0)/d_0$, where d_0 is the interplanar distance in the bulk, and i and j are the numbers of the corresponding atomic layers. Since the atoms of titanium and alumi-

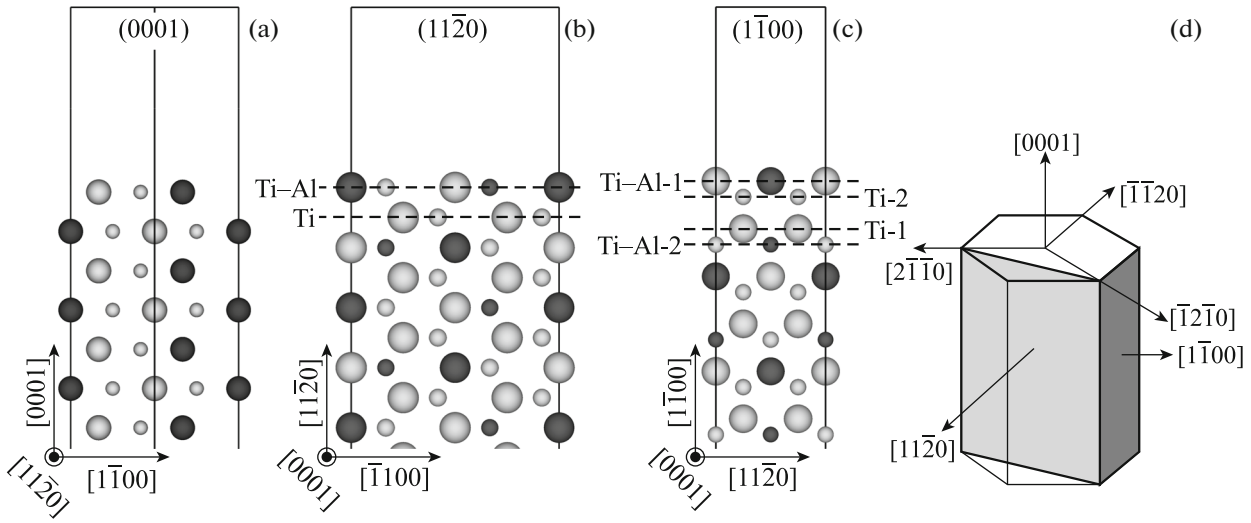

Fig. 2. Atomic structure of the low-index surfaces (a) (0001), (b) (11$\bar{2}$0), and (c) (1$\bar{1}$00) of the Ti_3Al alloy (side view) and (d) position of the corresponding crystallographic planes in the hexagonal cell of the alloy. Small and large balls show atoms lying in different planes. The designation of atoms is the same as in Fig. 1.

num are slightly shifted in the mixed layers, their average position was used to estimate the relaxation. It is seen that among the considered surfaces with the same orientation, those that have the lowest surface energy are also characterized by the least relaxation of the interlayer distances.

3.3. Adsorption of Oxygen on Low-Index Surfaces of Ti_3Al Alloy

3.3.1. Surface (0001). First, let us consider the adsorption of oxygen on the (0001) basal plane, as there are theoretical data [19, 20], which enable us to compare results. In addition, this is the only surface the atomic layers of that have a stoichiometric composition, and, according to the results obtained in [18], its energy decreases when aluminum is segregated to the surface. The positions at that the adsorption of oxygen on the (0001) surface was studied are shown in Fig 4a. Using the notation introduced in the earlier papers [15–17], we denote the top positions above the atoms of the surface layer by letter *T*; the positions at the center of the triangles formed by the surface atoms located above the atoms of the subsurface layer are denoted by *H*; and those positions under which there are no substrate atoms are denoted as *F*-positions. Note that in the *H*- and *F*-positions, the oxygen adatom is coordinated threefold by surface atoms. It is seen from Table 3, which presents the calculated adsorption energies, that the most preferred is the *F*1-position, where oxygen interacts with three surface titanium atoms. In this case, the O–Ti bond length is 1.95 Å. Recall that in TiO_2 with a rutile structure, the oxygen–titanium bond length is 1.96 Å. The adsorption energy in the H_{Al}-position is only slightly lower (Table 3) than in the *F*1-position. In the H_{Al}-position, the oxygen atom also interacts with three surface titanium atoms; the O–Ti bond length is 1.96 Å. The oxygen in this position is located above the subsurface aluminum atom, but the distance between them is much larger than the sum of the covalent radii. In this case, oxygen interacts with the aluminum atom through the hybridization of Al *s*, *p*-orbitals with *s*, *d*-orbitals of surface titanium atoms rather than directly. In *F*2- and H_{Ti}-positions, the appearance of aluminum in the nearest neighbors lowers the adsorption energy by ~0.9 eV. The latter is because the contribution from hybridization of O *p*-orbitals with Al *s*, *p*-orbitals to the binding energy is much smaller than that from the

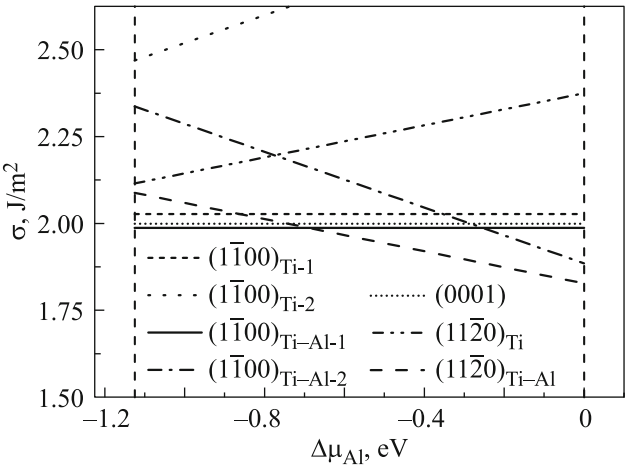

Fig. 3. Dependence of surface energies of low-index surfaces of Ti_3Al alloy on the chemical potential of aluminum.

Table 2. Relaxation of the first (Δd_{12}), the second (Δd_{23}), and the third (Δd_{34}) interlayer distances for pure Ti_3Al surfaces and splitting ε of the mixed layer closest to the surface

Parameter	Surface						
	(0001)	$(11\bar{2}0)_{Ti}$	$(11\bar{2}0)_{Ti-Al}$	$(1\bar{1}00)_{Ti\text{-}1}$	$(1\bar{1}00)_{Ti\text{-}2}$	$(1\bar{1}00)_{TiAl\text{-}1}$	$(1\bar{1}00)_{TiAl\text{-}2}$
Δd_{12}, %	−5.3	−8.2	−3.6	−15.5	−8.5	2.2	−12.4
Δd_{23}, %	1.0	−1.2	2.1	−2.1	−4.5	0.7	5.7
Δd_{34}, %	−1.8	1.7	0.3	2.6	−0.7	−1.6	2.4
ε, Å	0.19	0.07	0.03	0.22	−0.03	−0.07	0.10

The negative value of ε means that the titanium atom is located higher than the aluminum atom.

Table 3. Adsorption energy of oxygen E_{ads} on the $Ti_3Al(0001)$ surface, distance between oxygen and the nearest atoms of the substrate, d(O–*Me*), and position of oxygen h_0 relative to the surface layer (data [20] are given in brackets)

Parameter	Position					
	*F*1	*F*2	H_{Ti}	H_{Al}	T_{Ti}	T_{Al}
E_{ads}, eV	6.64	5.70	5.61	6.51	4.01	2.88
E_b, eV	9.19 (10.87)	8.26 (9.89)	8.17 (9.81)	9.07 (10.77)	6.57	5.44 (7.03)
d(O–Ti), Å	1.95 (1.94)	1.94 (1.92)	1.95 (1.93)	1.96 (1.94)	1.74	3.26
d(O–Al), Å	3.51	1.94 (1.96)	1.92 (1.95)	3.33	3.36	1.71 (1.71)
h_0, Å	0.99 (1.01)	1.06 (1.12)	0.96 (1.05)	1.00 (1.03)	1.69	1.51 (1.55)

hybridization of oxygen states with transition metal states. The lowest adsorption energies were obtained in the apical T_{Al}- and T_{Ti}-positions, since Al p_z- and Ti d_{z^2}-orbitals, ensuring interaction with oxygen in these positions, are practically unoccupied. Therefore, the interaction of oxygen with the surface in the top positions is less favorable, which is reflected by the obtained values of the adsorption energies (Table 3). Note that the preference for titanium-enriched positions for oxygen adsorption was also found in our earlier studies [15–17] for TiAl and $TiAl_3$ alloys.

The adsorption of oxygen significantly affects the atomic structure of the alloy surface. In practically all hollow (*F* and *H*) positions, the first interlayer distance (d_{12}) increases by 0.4–3.3%, whereas for a clean surface, a compression of the first interlayer distance by 5.3% is typical. Note that at the top T_{Al}-position, the negative relaxation of the surface is not removed, but, on the contrary, the compression of the first interlayer distance increases to 5.6%. In general, the relaxation of the following interlayer distances varies insignificantly.

Since the values of the binding energy were given in [20], we present these energies calculated using the spin-polarized energy of the oxygen atom (Table 3) to compare the results. It can be seen that the tendencies in the binding energy of oxygen to the (0001) surface coincide in both works, although the values of E_b themselves are significantly different. Note that, for example, in the *F*1-position, the difference between the total energies of the surface with oxygen and the clean surface is −10.75 eV, which agrees well with the value of −10.87 eV given in [20] as the binding energy. This allows us to assume that in [20], the value of the energy of the oxygen atom was used, which was obtained by the nonspin-polarized method. In this case, the energy of the oxygen atom is very small and can be neglected.

The fact that specific positions are more preferable for the adsorption of oxygen on the low-index surfaces of the Ti_3Al alloy can be explained by analyzing electronic characteristics. The local electronic densities of states (DOS) of oxygen and the nearest metal atoms for positions *F*1, H_{A1}, and T_{A1} are presented in Figs. 4b–4d. Since oxygen predominantly interacts with the metal atoms of the surface layer, this leads to the appearance of peaks on local DOS of Ti and Al, which coincide in the energy position with the corresponding peaks of O *s*, *p*-bands. It is seen that in the most energetically preferred *F*1-position, the *p*-band of oxygen has two narrow peaks located at energies of −5.2 and −4.7 eV. At the same energies, titanium states are located, which are split off from the bottom of the valence band of the metal because of its interaction with the *p*-states of oxygen, and a pseudogap is formed between titanium states at an energy of −4 eV (Fig. 4b). There is also a small peak of the DOS of titanium, localized at energies of −19.1 eV, caused by the hybridization of its states with *s*-states of oxygen. The sharp peak corresponding to the O *s*-band is at ener-

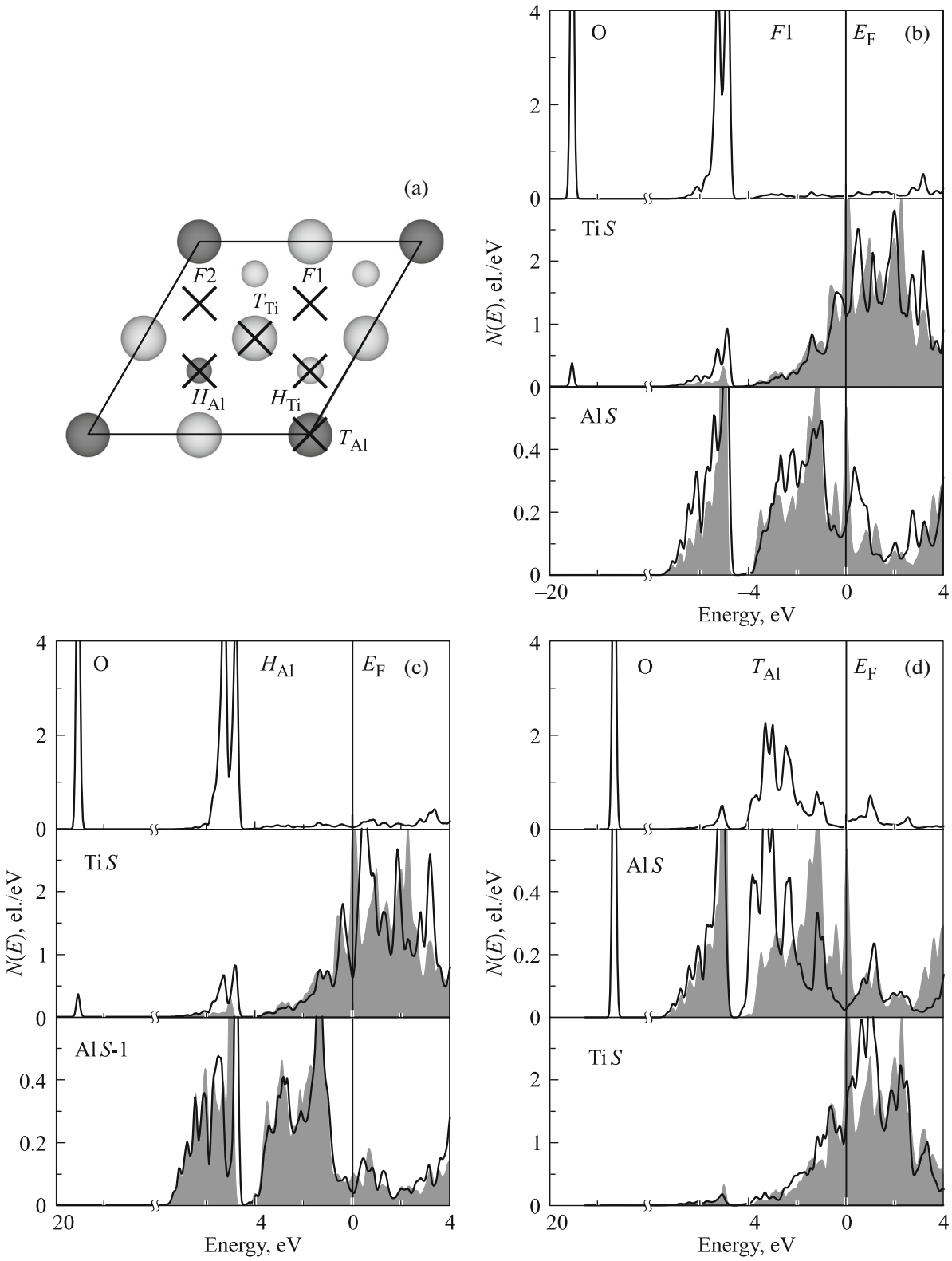

Fig. 4. (a) Positions of oxygen adsorption on the stoichiometric surface (0001) and local DOS of oxygen and the nearest atoms of the surface (*S*) and subsurface (*S*-1) layers for positions (b) *F*1, (c) H_{Al}, and (d) T_{Al}. Local DOS of Ti and Al atoms on the clean surface are shown in gray. The designation of Ti and Al atoms is the same as in Fig. 1. Atoms of the surface and subsurface layers are shown by large and small balls, respectively.

gies from −19.5 to −17 eV, depending on the position of oxygen adsorption on the alloy surface. The local DOS of the surface aluminum atom also change, but this is because of the hybridization of Al *s*, *p*-orbitals with *s*, *d*-orbitals of titanium atoms, with which oxygen is directly bound to the surface, rather than due to direct interaction with aluminum, since the O–Al interatomic distance is 3.51 Å. An estimate of charge transfer by the Bader method [45] showed that in the adsorption in the *F*1-position, a charge of 1.09*e* comes to the oxygen adatom, with the titanium atoms nearest to oxygen losing ~0.38*e*. In general, the appearance of new peaks, the change in the structure of the DOS curves of surface and subsurface metal atoms, their shift toward negative energies relative to the DOS of atoms on a clean surface, and the splitting of low-lying states indicate the formation of new metal–oxygen bonds and the weakening of metal bonds between the atoms of the surface layers. The DOS of those atoms that are directly involved in the interaction with oxygen change particularly strongly. This behavior is also typical for other adsorption positions.

The structure of the DOS of oxygen in its adsorption at the H_{Al}-position changes insignificantly. The difference lies in the stronger splitting of the oxygen *p*-band: the corresponding peaks lie at energies of −5.3 and −4.8 eV (Fig. 4c). The charge transfer to the adsorbed oxygen atom in this case is practically the same as in the *F*1-position. However, unlike the *F*1-position, the center of gravity of the O *s* band in the H_{Al}-position is shifted by 0.1 eV to the Fermi level, which may indicate a lower oxygen binding energy (by 0.13 eV) at this position. In addition, the O–Ti bond length is also 0.01 Å greater in the H_{Al}-position than in the *F*1-position. Note that the corresponding DOS curves of metallic atoms in the H_{Al}-position vary in the same way as described above. In addition, Fig. 4c shows the DOS of a subsurface aluminum atom, which change to a lesser degree than the DOS of surface aluminum atoms. Their change is similar to that shown in Fig. 4b; the corresponding graphs are not given.

The situation is fundamentally different when the oxygen atom is adsorbed in the top T_{Al}-position above the aluminum atom. It is seen that (Fig. 4d) that both *s*- and *p*-bands of oxygen shift substantially to the Fermi level, while the sharp peak of the *s*-band is much higher at energy (−17.3 eV) than in the other two positions. At the same energy, a sharp peak of the *s*-states of aluminum, induced by the interaction with oxygen, is located. As on a clean surface, the valence band of aluminum is split into *s*- and *p*-bands; the *p*-band of oxygen also splits into two subbands due to interaction. One small subband is located in the range from −6.2 to −4.8 eV, and another is at energies above −4.1 eV. It is seen that the position of all the peaks of the O *p*-band coincides with the corresponding peaks of Al *p*-states. Since the surface atoms of titanium are at a distance of 3.26 Å from the oxygen adatom, their DOS changes only slightly: in the energy range from −1.3 to −0.8 eV, additional states arise due to hybridization of Ti *s*, *d*-states with Al *p*-states. Thus, at this top position, oxygen interacts primarily with the *p*-states of surface aluminum, with the center of gravity of the *p*-band shifting by ~1 eV from the Fermi level.

The change of local DOS of surface atoms upon adsorption of oxygen in other hollow positions is similar to that described above for *F*1- and H_{Al}-positions. In contrast to the case of oxygen adsorption on the surfaces of alloys with a high aluminum concentration [10, 11, 13–17], the adsorption energy on the surface of $Ti_3Al(0001)$ depends to a lesser degree on the position of the oxygen adatom. The scatter in the binding energies for the four hollow positions is only ~1 eV, and the larger adsorption energy in the T_{Ti}-position than in the T_{Al}-position can be explained by the greater hybridization of the oxygen *p*-orbitals with the *d*-orbitals of the transition element atom. It is this factor that due to an increase in the concentration of titanium on the (0001) surface leads to an increase in the binding energy of oxygen at a given surface compared with that on the stoichiometric surfaces of the TiAl and $TiAl_3$ alloys.

3.3.2. Surface $(11\bar{2}0)$. It is found for the atomic structure of the $Ti_3Al(11\bar{2}0)_{Ti-Al}$ surface with a mixed termination (Fig. 2b) that it is stable in the aluminum-enriched region. First, a few words need to be said about the packing density of all three surfaces under study. In the case of surface (0001), the packing density is 0.140 $Å^{-2}$, while for surfaces $(11\bar{2}0)$ and $(1\bar{1}00)$, it is much smaller: 0.087 and 0.075 $Å^{-2}$, respectively. The more densely packed surfaces are usually characterized by a lower surface energy, whereas in this case, the chemical composition of the surface layer, namely, the larger concentration of aluminum atoms in this layer, was decisive. It was also noted in [18] that an increase in the concentration of aluminum on the surface of the alloy lowered the surface energy.

It is seen from Fig. 5a that there are a large number of nonequivalent positions on the $(11\bar{2}0)$ surface, which must be considered in the study of oxygen adsorption. In addition to the previously mentioned hollow and top positions, there are also stable bridge *B*-positions between the two surface atoms. The highest oxygen adsorption energy on this surface is 5.58 eV (Table 4) and corresponds to the *H*1-position in the titanium triangle above the subsurface titanium atom. Adsorption of oxygen in this position leads to a displacement of the nearest surface titanium atoms by 0.10–0.12 Å towards the vacuum, and the aluminum atom, which is located at a distance of 2.65 Å, is shifted by 0.05 Å. The lengths of the oxygen bonds with two surface titanium atoms are by 0.42 Å greater than that with the nearest surface titanium atom (1.98 Å), whereas the distance to the subsurface titanium atom is 2.07 Å. Obviously, the interaction of

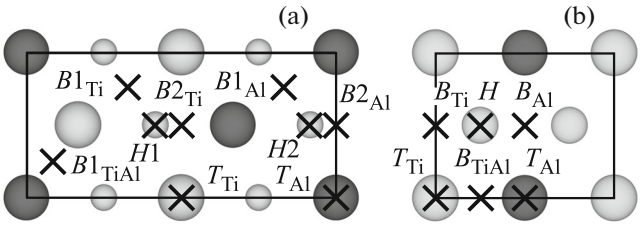

Fig. 5. Positions of oxygen adsorption on (a) $(11\bar{2}0)_{Ti-Al}$ and (b) $(1\bar{1}00)_{Ti-Al-1}$ surfaces with a mixed termination. The designation of Ti and Al atoms is the same as in Fig. 4a.

oxygen with the latter atoms is stronger than with the other two.

When oxygen is adsorbed in the $B2_{Ti}$-position of the long bridge, oxygen is more strongly bound to the subsurface titanium atom (2.05 Å) and surface aluminum atom (1.89 Å) than to two titanium atoms in the surface layer (2.35 Å). Namely this structural factor caused a lower value of the oxygen adsorption energy in the $B2_{Ti}$-position than in the $H1$-position. Note that the $H2$-position, in which oxygen is located in the center of the aluminum triangle above the titanium atom of the second layer, is unstable, because in the process of relaxation, oxygen from this position is shifted to the bridge $B2_{Al}$-position. In the latter case, the distance to the nearest surface titanium atom (1.91 Å) is only 0.07 Å smaller than to the subsurface titanium, but it is substantially smaller than to the surface aluminum atoms (2.39 Å). The length of the O–Ti bonds in this case is less than in the adsorption of oxygen in the $H1$ and $B2_{Ti}$ positions, but it interacts with a smaller number of titanium atoms in the $B2_{Al}$-position, which results in a lower binding energy. As on the $Ti_3Al(0001)$ surface, the lowest adsorption energy is found in the top T_{Al}-position. The interatomic (O–*Me*) distances for all positions are given in Table 4.

Despite the small difference in the oxygen adsorption energies in the $H1$ and $B2_{Ti}$ positions, the local DOS of oxygen adatom and surface atoms demonstrate different mechanisms of chemical bonding of oxygen to the surface (Figs. 6a and 6e). The DOS of surface titanium atoms during adsorption of oxygen in the $H1$-position change in the same way as noted earlier for the hollow positions: low-lying states split off from the bottom of the titanium valence band arise due to interaction with the *s* and *p* oxygen bands (Fig. 6a) even on the DOS curves corresponding to titanium atoms more distant from oxygen. Although the O–Al distance is 0.74 Å exceeds the sum of the covalent radii of oxygen and aluminum, the DOS of the surface aluminum atom varies significantly. However, these changes affect largely the *s*-state of aluminum, while the sharp peak located below –5 eV, characteristic of a clean surface, splits into two peaks, which is clearly seen in Fig. 6b. This behavior is observed when hydrogen interacts with impurity atoms of boron, aluminum, or gallium in alloys [46] and at their grain boundaries [47]. In the aforementioned papers, this is explained by the Pauli exclusion principle, since hybridization of the s^2-states of the impurity and the s^1-state of hydrogen takes place, which leads to the formation of antibonding states (an additional peak of DOS at slightly higher energies than the first peak) and mutual repulsion between atoms. Hybridization of $2s^2$-states of oxygen with $3s$-states of aluminum can also lead to a similar effect. This argument is supported by the fact that the aluminum atom undergoes a lateral displacement (by ~0.1 Å) away from the oxygen adatom in the $H1$-position in comparison with its position in the case of a clean surface. In addition, the localization of the states of the low-energy peak clearly indicates their binding nature, while the higher-energy states do not contribute to the bond of oxygen to aluminum (Figs. 6c and 6d). In general, the strong interaction of the $2p$-orbitals of oxygen with the *s*, *d*-orbitals of the three surface and one subsurface titanium atoms causes the maximum adsorption energy in the $H1$-position.

When oxygen is adsorbed in the $B2_{Ti}$-position (Fig. 6e), the Al *p*-states also undergo significant changes, while the fine structure of the DOS in the energy range from –7.3 to –4.5 eV is in good agreement with the structure of the oxygen *p*-band. In addition, the sharp peak at an energy of –4.6 eV on the alu-

Table 4. Adsorption energy of of oxygen E_{ads} on the $Ti_3Al(11\bar{2}0)_{Ti-Al}$ surface, distance between oxygen and atoms of the substrate d(O–*Me*), and position of oxygen h_0 relative to the surface layer

Parameter	Position							
	$H1$	$B1_{Ti}$	$B1_{Al}$	$B1_{TiAl}$	$B2_{Ti}$	$B2_{Al}$	T_{Ti}	T_{Al}
E_{ads}, eV	5.58	5.41	5.17	5.39	5.50	5.10	3.90	2.46
d(O–Ti), Å	1.98, 2.07*	1.86, 3.30*	3.89, 2.04*	1.93, 2.06*	2.35, 2.05*	1.91, 1.98*	1.69, 4.15*	3.35, 3.90*
d(O–Al), Å	2.65	3.81	1.97	1.85	1.89	2.39	3.70	1.67
h_0, Å	0.44	1.17	0.07	0.52	0.40	0.50	1.69	1.54

*The distance from the oxygen adatom to the atoms of the subsurface layer.

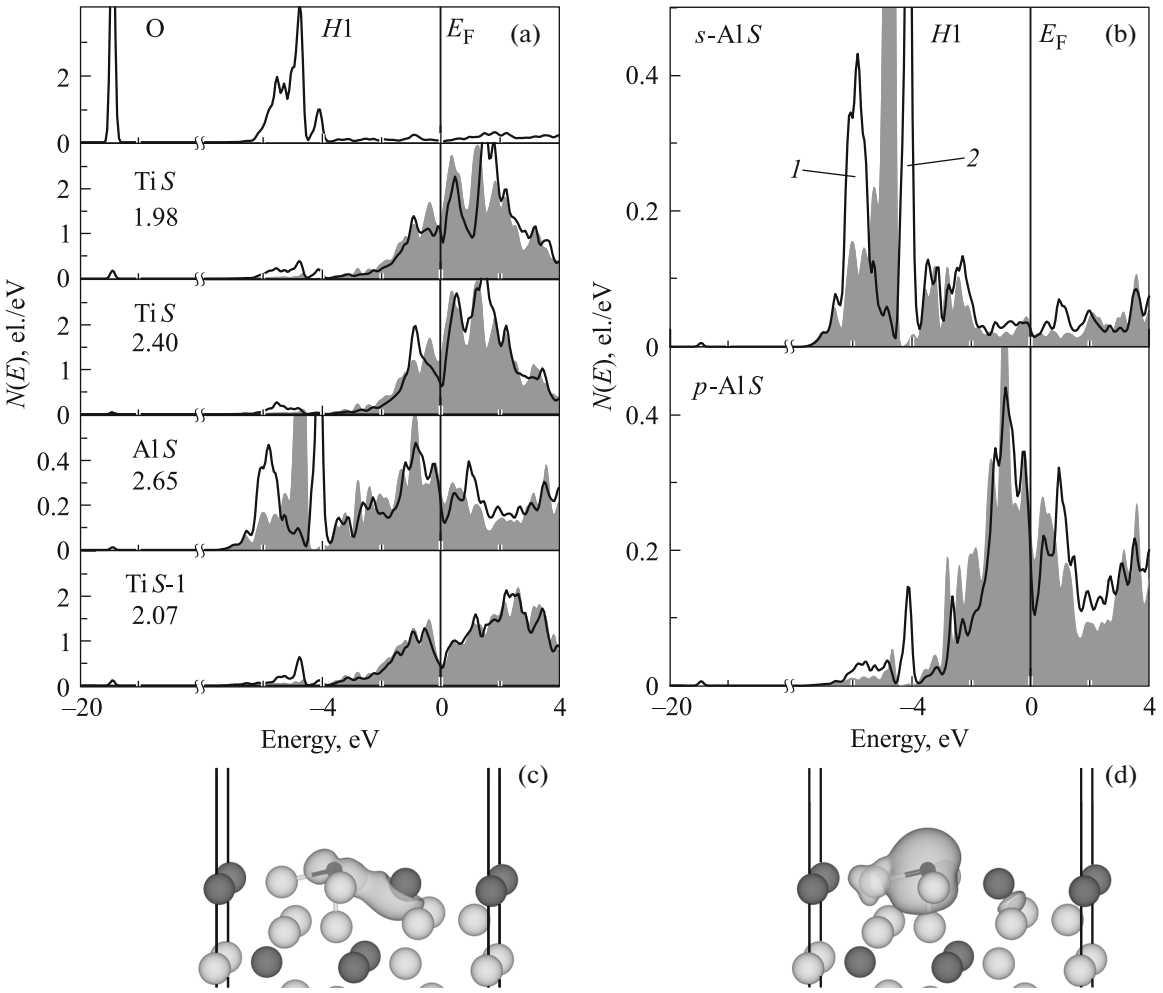

Fig. 6. Local densities of the electronic states of oxygen and the nearest atoms of the surface (*S*) or subsurface (*S*-1) layer in the adsorption of oxygen at positions (a) *H*1 and (e) $B2_{Ti}$ on the $Ti_3Al(11\bar{2}0)_{Ti-Al}$ surface and (b and f) partial DOS of the surface aluminum atom for the same positions of oxygen adsorption. The corresponding DOS of atoms of the clean surface are shown in gray. The numbers on parts (a and e) are the O–*Me* bond lengths (Å). Localization of the states marked with *1* and *2* in parts (b and f) is shown in parts (c and g) and (d and h), respectively.

minum DOS for a clean surface shifts by 1.7 eV toward negative energies upon interaction with oxygen. We also note a peak centered at an energy of –3.8 eV, which appears due to a decrease in the number of states near the Fermi energy. The low-energy peak, located much lower (–19.3 eV), is caused by the interaction of Al *s*, *p*-states with the *s*-band of oxygen (Fig. 6f). We note that the peak of the *s*-states of aluminum at an energy of –6.3 eV (Fig. 6f, peak *1*) has practically the same localization as the corresponding peak in the adsorption of oxygen in the *H*1-position. At the same time, the sharp peaks of the Al *s*, *p*-states (Fig. 6f, peaks *2*) at an energy of –3.8 eV are also due to hybridization with the O *p*-states. In this case, the surface aluminum atom does not undergo lateral displacement. As it is seen from Fig. 6h, the localization of states situated in this energy range (from –4.2 to –3.4 eV) (Fig. 6f) corresponds mainly to the p_z-orbitals of oxygen.

Thus, when oxygen is adsorbed in the $B2_{Ti}$-position, the contributions of the subsurface titanium atom and surface aluminum atom do not compensate completely the decrease in the binding energy of oxygen to the titanium atoms of the surface layer due to the increase in the distance between them. The change in the DOS curves in the adsorption in top positions is similar to that noted earlier on the (0001) surface and therefore is not discussed. In general, the scatter in the adsorption energies on the $Ti_3Al(11\bar{2}0)_{Ti-Al}$ surface is even smaller (~0.5 eV) than at the (0001) surface, and it indicates a decrease in the selectivity of the oxygen interaction on the surface.

3.3.3. Surface $(1\bar{1}00)$. On the $(1\bar{1}00)_{Ti-Al-1}$ surface, adsorption of oxygen was considered in the posi-

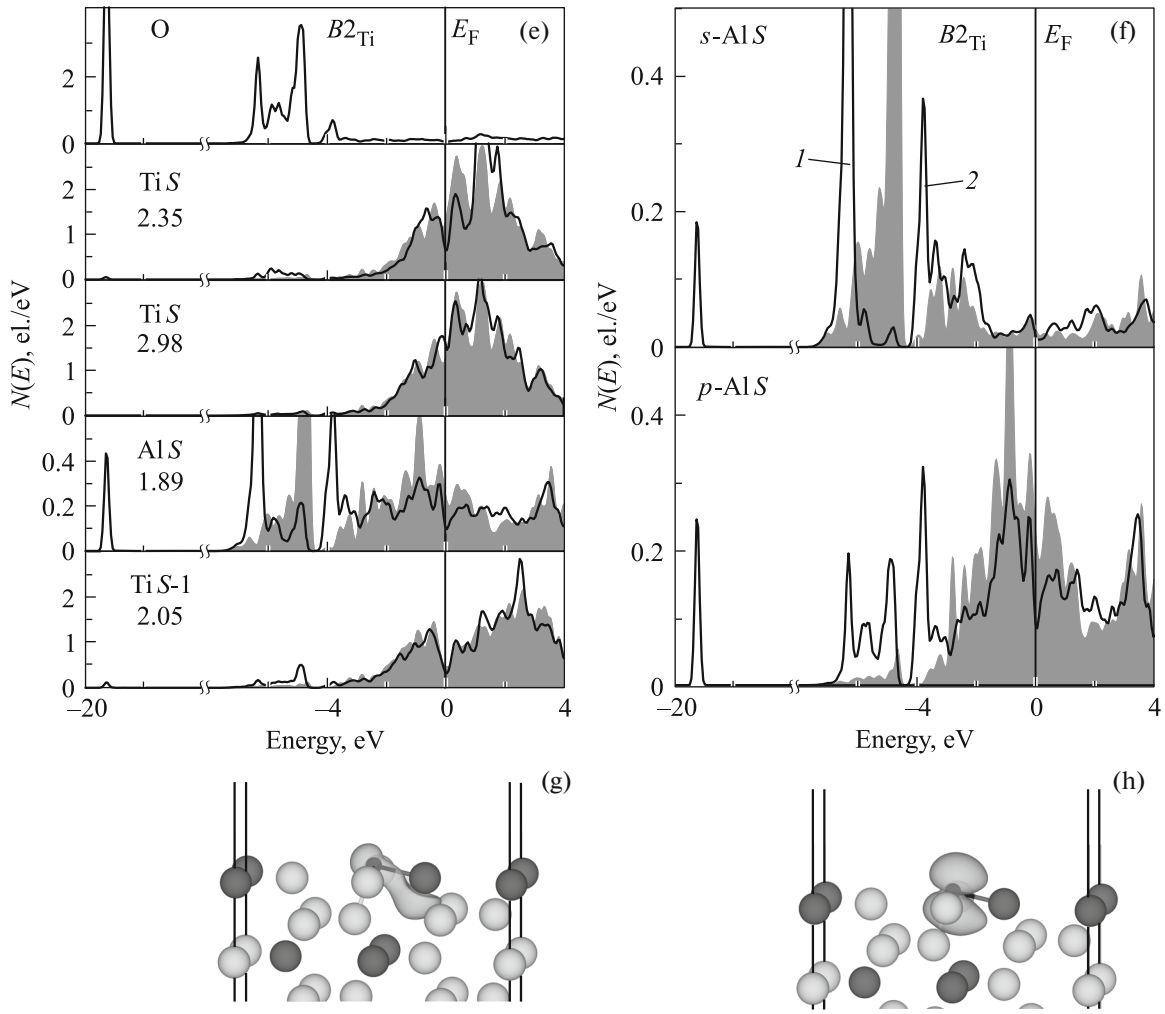

Fig. 6. (Contd.)

tions shown in Fig. 5b. It turns out that the hollow H-position in the center of the rectangle with a composition containing the same amounts of titanium and aluminum over the subsurface titanium atom is not stable, since oxygen shifts to the bridge B_{Ti}-position (Table 5). In this B_{Ti}-position, it forms a chemical bond mainly with two titanium atoms of the subsurface layer, the distance to which is 0.4 Å smaller than to the titanium atoms of the surface layer. This conclusion is confirmed by calculations of the local DOS of the surface and subsurface titanium atoms (Fig. 7a). It is seen that the electronic structure of the subsurface titanium atoms during adsorption of oxygen changes more than that of the surface layer: the structure of low-lying peaks of the DOS of titanium atoms is more pronounced in the former case, and a larger number of states is split off from the bottom of the titanium valence band. Since aluminum atoms are located at a considerable distance from oxygen (3.72 Å), their DOS do not change (Fig. 7a).

The bridge B_{TiAl}-position is second-preferable (the adsorption energy is 1.57 eV lower), but the orientation of this bridge (along the $[11\bar{2}0]$ direction) differs from the orientation of the titanium bridge in the previous case (along he [0001] direction). In this case, the atoms of titanium and aluminum of the surface layer were initially located much closer (by 1.77 Å) to each other than the titanium atoms in the B_{Ti}-position. The adsorption of oxygen at the position of the mixed bridge leads to a different displacement of the Al and Ti atoms towards the vacuum (by 0.11–0.21 Å), with titanium atoms locating above the aluminum atoms by 0.16 Å. In addition, a lateral displacement of the atoms by ~0.1 Å is observed in the direction toward each other. It is seen that the O p-band splits as a result of interaction with the nearest surface atoms (Fig. 7b); the first small peak located at –5.8 eV is mainly due to the interaction with the s-states of aluminum, while in the region of the double peak (from –4.7 to –3.5 eV), oxygen mainly interacts with Ti d- and Al p-states. The DOS curves of subsurface titanium atoms indicate that

Table 5. Adsorption energy of of oxygen E_{ads} on the $Ti_3Al(1\bar{1}00)_{Ti-Al-1}$ surface, distance between oxygen and atoms of the substrate $d(O-Me)$, and position of oxygen h_0 relative to the surface layer

Parameter	Position				
	B_{Ti}	B_{Al}	B_{TiAl}	T_{Ti}	T_{Al}
E_{ads}, eV	6.41	4.70	4.84	3.50	2.57
d(O–Ti), Å	2.33, 1.93*	3.73, 1.92*	1.84, 3.25*	1.69, 3.90*	3.15, 3.77*
d(O–Al), Å	3.72	2.35	1.79	3.44	1.68
h_0, Å	0.24	0.37	1.08	1.69	1.31

*The distance from the oxygen adatom to the atoms of the subsurface layer.

these atoms are practically not involved in the interaction with oxygen, and small changes in the DOS near the Fermi level reflect an indirect interaction through hybridization with surface metallic atoms.

A much smaller value of the adsorption energy (by 1.71 eV) for the B_{Al}-position than for the B_{Ti}-position is a reflection of the fact that the surface aluminum atoms interact more weakly with oxygen than titanium atoms. Recall that delocalized 3*s*- and 3*p*-states are more strongly displaced by interaction with oxygen than localized *d*-orbitals (Fig. 7c); however, the hybridization of O *s*, *p*–Ti *d* is stronger than O *s*, *p*–Al *s*, *p*. The interaction with the subsurface titanium atoms, which are located at the same distance from oxygen in both positions, is almost similar, and the DOS curves reflect this (Figs. 7a and 7c). The mechanism of interaction in the top positions on the surface is practically independent of the orientation of the surface. Thus, the large energy of adsorption of oxygen in the B_{Ti}-position is due to the fact that in this position, oxygen interacts with two titanium atoms of both the surface and subsurface layers, whereas in other positions, the number of nearest titanium atoms decreases, and the replacement of one of the atoms by an aluminum atom, as in the B_{TiAl}-position, lowers the binding energy of oxygen due to a decrease in the hybridization of O *s*, *p*–Al *s*, *p* contribution.

Since the other terminations of the $(11\bar{2}0)$ and $(1\bar{1}00)$ surfaces of the Ti_3Al alloy are not stable, adsorption of oxygen on them is not discussed. Note that the adsorption energy increases for the surfaces with a high titanium concentration in the surface and subsurface layers. On the contrary, on the $Ti_3Al(1\bar{1}00)_{Ti-Al-2}$ surface the adsorption energy in the bridge B_{Ti}- and B_{Al}-positions decreases somewhat, because in this case, the oxygen adatom is located above one of the subsurface atoms (Al or Ti) rather than interacts with two subsurface titanium atoms. Such interaction, as calculations for top positions show, is energetically less advantageous.

3.4. Concluding Remarks

Thus, our calculations show that on all three low-index surfaces of the Ti_3Al alloy considered, the maximum binding energies of oxygen correspond to its adsorption in titanium-enriched positions. This should promote the formation of titanium oxides on the Ti_3Al surface. Indeed, as shown in a number of publications [48, 49], titanium oxidation is observed at room temperature and precedes the oxidation of aluminum on the surface of both Ti_3Al and TiAl. The greater solubility of oxygen in the Ti_3Al alloy than in other alloys is attributed to the advantage of introducing oxygen into the octahedral positions (Ti_6) with titanium in the nearest neighbors. For example, in the TiAl alloy, there are only positions containing two and four aluminum atoms (Al_2Ti_4 and Al_4Ti_2). The adsorption energy in the $O1$-position (Ti_6) in the Ti_3Al alloy is ~2.2 eV higher than that in the corresponding octahedral position (Al_2Ti_4) in TiAl [15, 16]. At the same time, at a high temperature, a thin layer (~0.2–0.5 nm) of aluminum oxide [21] is formed on the Ti_3Al surface, which corresponds to an oxide film containing two to five atomic layers of oxygen. This behavior supposes a surface segregation of Al, which enables adsorbed oxygen to interact with aluminum [21]. A small thickness suggests the formation of islands that grow laterally on the surface rather than a continuous film of aluminum oxide. As noted above, an increase in the aluminum concentration in the surface layer leads to a decrease in surface energy irrespective of the orientation of the surface of the Ti_3Al alloy. Direct estimates of the effect of aluminum segregation on the surface energy of $Ti_3Al(0001)$, carried out in [18], also confirmed that the formation of antistructural defects of aluminum in the surface layer is energetically favorable. In addition, according to the data of [18], the adsorption of oxygen also contributes to the segregation of aluminum. The activation energies of the self-diffusion of Al and Ti in Ti_3Al are 395 and 288 kJ/mol (4.09 and 2.99 eV) [50]. It is obvious that the growth of aluminum oxide on the surface of the alloy is limited by the flow of aluminum atoms to the surface. Moreover, aluminum diffusion requires the presence of alu-

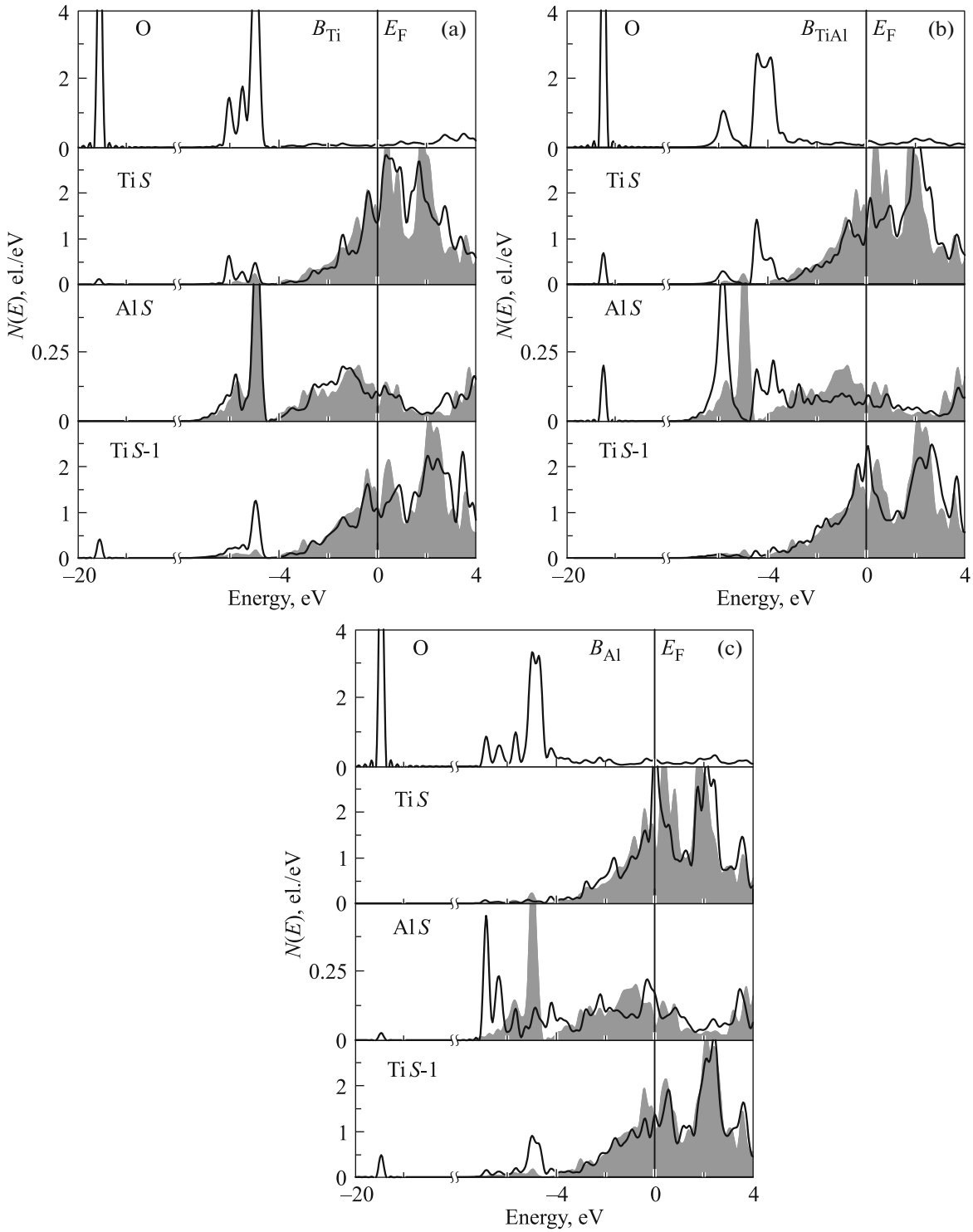

Fig. 7. Local densities of the electronic states of oxygen and the nearest atoms of the surface (*S*) or subsurface (*S*-1) layer in the adsorption of oxygen at positions (a) B_{Ti}, (b) B_{TiAl}, and (c) B_{Al}. The corresponding DOS of atoms of the clean surface are shown in gray.

minum vacancies at the alloy–oxide interface. The latter leads to the formation of a titanium-enriched region. It is believed that a decrease in the number of Al–Ti bonds in this region increases the activity of titanium, and the defectiveness of the film of aluminum oxide enables it to diffuse to the surface where its

oxidation occurs. Thus, experiment [21] reveals the formation of a titanium oxide film over a thin, highly defective aluminum oxide film. Our simulation of the adsorption of oxygen on the $Ti_3Al(0001)$ surface with antistructural Al defects in the surface layer shows that oxygen interacts with aluminum at low concentrations, and with an increase in oxygen concentration, the titanium atoms shift to the surface where they are coordinated by oxygen, as in TiO_2. Practically similar behavior was observed at the mixed termination of the $TiAl_3(001)$ surface in our previous paper [17].

In conclusion, although direct simulation of high-temperature oxidation of the Ti–Al alloy surface is difficult in the framework of the DFT, these methods, which give information for the ground state of alloys, are intensively used to study the adsorption of oxygen. It is believed that in order to understand the mechanisms of high-temperature oxidation of the surface, it is necessary to identify the main tendencies of the interaction of oxygen with the atoms in the surface layers, which are determined by the electronic subsystem and are practically independent of temperature.

4. CONCLUSIONS

The paper presents the results of calculations of oxygen adsorption in the bulk and on the low-index surfaces of the Ti_3Al alloy performed by the projector augmented-wave method in the framework of the density functional theory. It is shown that the adsorption of oxygen in the bulk of the alloy is most preferable at the titanium-enriched octahedral $O1$-position. This conclusion is valid for all titanium aluminides [15–17, 39] and agrees with the available experimental data [40].

Calculations of the surface energies of the low-index surfaces of the Ti_3Al alloy showed that the $(11\bar{2}0)_{Ti-Al}$ surface with a mixed termination is stable in the Al-enriched region, whereas the $(1\bar{1}00)_{Ti-Al\text{-}1}$ surface with a mixed termination is more stable in Ti-enriched limit. The difference in the surface energies of this structure and the (0001) basal surface is only 0.012 J/m^2, which is at the limit of the calculation accuracy. It is shown that on the stoichiometric $Ti_3Al(0001)$ surface, the most preferable position for oxygen adsorption is a threefold coordinated $F1$-position in that oxygen interacts with three surface titanium atoms. On the $Ti_3Al(11\bar{2}0)_{Ti-Al}$ surface with a mixed termination, oxygen is preferentially adsorbed in the $H1$-position at the center of the titanium triangle, while for the bridge B_{Ti}-position is found to be more preferable on the $(1\bar{1}00)_{Ti-Al\text{-}1}$ surface. In general, the results demonstrate an increase in the oxygen adsorption energy with an increase in the titanium concentration in the nearest environment of oxygen and with an increase in the titanium concentration in Ti–Al alloys. In the present work, only the microscopic aspect of the interaction of oxygen on low-index surfaces is considered. Although many effects are not taken into account in the calculations, including temperature, structural transformations on the surface, and others, nevertheless, calculations from the first principles enable us to estimate quite correctly the binding energy of oxygen in the bulk and on the surface and to obtain information on the initial stage of oxidation.

ACKNOWLEDGMENTS

This work was supported by the Russian Foundation for Basic Research, project no. 14-02-91150-GFEN; partially performed in the framework of the program of Institute of Strength Physics and Materials Science, Siberian Branch, Russian Academy of Sciences, project no. 23.1.2; and supported by the Competitiveness Improvement Program of Tomsk State University.

Numerical calculations were performed using a SKIF–Cyberia supercomputer at Tomsk State University and with the help of the resources of the supercomputer complex of the Moscow State University.

REFERENCES

1. Z. Li and W. Gao, in *Intermetallics Research Progress*, Ed. by Y. N. Berdovsky (Nova Science, New York, 2008), p. 1.
2. I. Polmear, *Light Alloys: From Traditional Alloys to Nanocrystals* (Elsevier, Amsterdam, 2005, Tekhnosfera, Moscow, 2008).
3. F. H. Froes, C. Suryanarayana, and D. Eliezer, J. Mater. Sci. **27**, 5113 (1992).
4. Y. Umakoshi, M. Yamaguchi, T. Sakagami, and T. Yamane, J. Mater. Sci. **24**, 1599 (1989).
5. F. Dettenwanger and M. Schütze, Oxid. Met. **54**, 121 (2000).
6. R. G. Reddy, JOM **54**, 65 (2002).
7. M. P. Brady and P. F. Tortorelli, Intermetallics **12**, 779 (2004).
8. J. G. Speight, *Lange's Handbook of Chemistry*, 16th ed. (McGraw-Hill, New York, 2005), p. 124.
9. A. Y. Lozovoi, A. Alavi, and M. W. Finnis, Phys. Rev. Lett. **85**, 610 (2000).
10. H. Li, S. Wang, and H. Ye, J. Mater. Sci. Technol. **25**, 569 (2009).
11. S.-Y. Liu, J.-X. Shang, F.-H. Wang, and Y. Zhang, Phys. Rev. B **79**, 075419 (2009).
12. L. Wang, J.-X. Shang, F.-H. Wang, Y. Zhang, and A. Chroneos, J. Phys.: Condens. Matter **23**, 265009 (2011).
13. Y. Song, J. H. Dai, and R. Yang, Surf. Sci. **606**, 852 (2012).
14. L. Wang, J.-X. Shang, F.-H. Wang, Y. Chen, and Y. Zhang, Acta Mater. **61**, 1726 (2013).
15. S. E. Kulkova, A. V. Bakulin, Q. M. Hu, and R. Yang, Comput. Mater. Sci. **97**, 55 (2015).

16. A. V. Bakulin, C. E. Kulkova, Q. M. Hu, and R. Yang, J. Exp. Theor. Phys. **120**, 257 (2015).
17. A. M. Latyshev, A. V. Bakulin, S. E. Kulkova, Q. M. Hu, and R. Yang, J. Exp. Theor. Phys. **123**, 991 (2016).
18. S.-Y. Liu, S. Liu, D. Li, T. M. Drwenski, W. Xue, H. Dang, and S. Wang, Phys. Chem. Chem. Phys. **14**, 11160 (2012).
19. L.-J. Wei, J.-X. Guo, X.-H. Dai, Y.-L. Wang, and B.-T. Liu, Surf. Rev. Lett. **22**, 1550053 (2015).
20. L.-J. Wei, J.-X. Guo, X.-H. Dai, L. Guan, Y.-L. Wang, and B.-T. Liu, Surf. Interface Anal. **48**, 1337 (2016).
21. V. Maurice, G. Despert, S. Zanna, P. Josso, M.-P. Bacos, and P. Marcus, Acta Mater. **55**, 3315 (2007).
22. P. E. Blöchl, Phys. Rev. B **50**, 17953 (1994).
23. G. Kresse and J. Joubert, Phys. Rev. B **59**, 1758 (1999).
24. G. Kresse and J. Hafner, Phys. Rev. B **48**, 13115 (1993).
25. G. Kresse and J. Furthmüller, Phys. Rev. B **54**, 11169 (1996).
26. G. Kresse and J. Furthmüller, Comp. Mater. Sci. **6**, 15 (1996).
27. J. P. Perdew, K. Burke, and M. Ernzerhof, Phys. Rev. Lett. **77**, 3865 (1996).
28. H. J. Monkhorst and J. D. Pack, Phys. Rev. B **13**, 5188 (1976).
29. H. Shi and C. Stampfl, Phys. Rev. B **76**, 075327 (2007).
30. K. P. Huber and G. Herzberg, *Molecular Spectra and Molecular Structure IV: Constants of Diatomic Molecules* (Van Nostrand Reinhold, New York, 1979).
31. Y. L. Liu, L. M. Liu, S. Q. Wang, and H. Q. Ye, Intermetallics **15**, 428 (2007).
32. M. H. Yoo, J. Zou, and C. L. Fu, Mater. Sci. Eng. A **192–193**, 14 (1995).
33. W. B. Pearson, *A Handbook of Lattice Spacing and Structures of Metals and Alloys*, 1st ed. (Pergamon, New York, 1958).
34. K. Tanaka. K. Okamoto, H. Inui, Y. Minonishi, M. Yamaguchi, and M. Koiwa, Philos. Mag. A **73**, 1475 (1996).
35. F. D. Murnaghan, Proc. Natl. Acad. Sci. USA **30**, 244 (1944).
36. T. Hong, T. J. Watson-Yang, X.-Q. Guo, A. J. Freeman, T. Oguchi, and J.-H. Xu, Phys. Rev. B **43**, 1940 (1991).
37. D. Sornadurai, B. Panigrahi, and Ramani, J. Alloys Compd. **305**, 35 (2000).
38. D. Music and J. M. Schneider, Phys. Rev. B **74**, 174110 (2006).
39. Y. Wei, H.-B. Zhou, Y. Zhang, G.-H. Lu, and H. Xu, J. Phys.: Condens. Matter **23**, 225504 (2011).
40. C. Y. Jones, W. E. Luecke, and E. Copland, Intermetallics **14**, 54 (2006).
41. R. Hultgren, P. D. Desai, M. Gleiser, and D. T. Hawkins, *Selected Values of Thermodynamic Properties of Binary Alloys* (Am. Soc. Metals, Metals Park, OH, 1973).
42. F. R. de Boer, R. Boom, W. C. M. Mattens, A. R. Miedema, and A. K. Niessen, *Cohesion in Metals: Transition Metal Alloys* (North Holland, Amsterdam, 1989).
43. *Smithells Metals References Book,* Ed. by E. A. Brandes and G. B. Brook, 7th ed. (Butterworth-Heinemen, London, 1992).
44. L. Wang, J.-X. Shang, F.-H. Wang, and Y. Zhang, Appl. Surf. Sci. **276**, 198 (2013).
45. G. Henkelman, B. P. Uberuaga, and H. Jónsson, J. Chem. Phys. **113**, 9901 (2000).
46. T. I. Spiridonova, A. V. Bakulin, and S. E. Kul'kova, Phys. Solid State **57**, 1921 (2015).
47. S. E. Kulkova, A. V. Bakulin, S. S. Kulkov, S. Hocker, and S. Schmauder, Phys. Scripta **90**, 094010 (2015).
48. M. R. Shanabarger, Mater. Sci. Eng. A **153**, 608 (1992).
49. M. R. Shanabarger, Appl. Surf. Sci. **134**, 179 (1998).
50. J. Rüsing and C. Herzig, Intermetallics **4**, 647 (1996).

Translated by O. Zhukova